Optimisation of a Solar Farm

George Gunn
Subsystem 1:
Battery Storage

Julian Syn
Subsystem 2:
Cooling System

Harry Schlote
Subsystem 3:
Farm Layout

Abstract

This report is a documentation of the optimisation of a solar farm, which aims to power a self-sustaining compound of 50 houses in Egypt. The global goal was to maximise the efficiency of the farm in relation to the cost. To achieve this, the problem was split into three subsystems – panel cooling system, the solar farm battery energy storage, and the layout of panels in the farm.

The outcome for the cooling system was $|-137930| W/m^2$ in efficiency saving roughly £19,274. The BESS will generate a 23% profit over its lifecycle amounting to $24,753 whilst ensuring energy can be used whilst the sun isn't shining. The area required for the layout of the panels was found to be $450m^2$ to meet the compounds power requirement of 500kWh per day (1).

1. Introduction

Egypt is ranked 7th in the world (2) for up-and-coming technology and development. As a developing country, providing energy to its own population should be a priority. Solar farms are an obvious solution to this problem since Egypt get about 100mm of rainfall each year (3). Additionally with the effects of climate change becoming more severe it is crucial to transition away from fossil fuels. However, with limited financial resources, designing a solar farm that allows for as little investment and maintenance as possible while providing enough electricity for an Egyptian compound of 50 homes is a challenge.

2. System-level problem and Subsystem Breakdown

To optimise maximum efficiency and minimise cost for a solar farm system in an Egyptian village, we identified 4 factors that have an effect. Adding Battery storage optimisation will improve efficiency of the system storing excess power for later use. The layout of the farm could be optimised to reduce land costs and boost energy production. As Egypt is a tropical country with a blazing sun, solar panels would work best at cooler temperatures hence the addition of a cooling system will improve panel efficiency. The system was initially decomposed with 4 subsystems to include location. The content relating to location is excluded from this report and is to be accessed separately.

Global optimisation formulation

Maximise $\mathbf{CE_{farm}} = \mathbf{CE_{layout}} + \mathbf{CE_{BESS}} + \mathbf{CE_{cooling}}$

$\mathbf{CE_{layout}}$ = Panel efficiency / (Land cost + Panel cost)

$\mathbf{CE_{BESS}}$ = Energy Saved / Battery cost over life

$\mathbf{CE_{cooling}}$ = Panel ΔT / system cost + running cost

Further analysing the global objective, it is clear the entire system is too complex to optimise efficiently. Each factor affecting system efficiency requires differing branches of mathematics and optimisation approaches due to differing variable categories and objective function complexity. As such a sub system level approach has been adopted. The Farm has been broken down into individual subsystems as shown in figure 1. Each subsystem will be optimised individually, subject to global constraints and requirements.

The cooling system will be optimised for efficiency by minimising heat flux with regards to length, diameter and thickness of the water pipes and velocity of water within the pipes.

To meet the energy requirements of the compound, the farm should contain substantial number of panels although the amount of space should be kept to a minimum. This will be done though optimising the panel height and its angle, the distance between rows and the number or rows themself.

A battery energy storage system will enable the farm to store surplus energy when the supply exceeds the demand. Then release it later, when demand exceeds the supply, for example when it is dark. The battery system will be optimised to maximise profit when compared to buying energy from the grid whilst ensuring the capacity is sufficient to satisfy the needs of the 50 houses.

Interdependencies

The main interdependency identified is between the Layout of the farm and the BESS. Layout will affect the power output from the PV array and thus impact one of the main parameters in the BESS design. This has been accounted for by setting global parameters of 50 houses with a total consumption of 500kWh per day. Additionally, the PV array output data used in the BESS optimisation will be for a generic solar installation layout. Optimising the layout will produce a greater PV output and as such the BESS will still be sufficient to meet requirements. The cooling system will increase the efficiency of the PV panels and thus impact layout and BESS optimisation parameters. The proportionate increase in efficiency does not impact the constraints in the layout subsystem. Additionally, the size of the BESS capacity will be based on residential demand decoupling it from supply. A battery can only discharge what energy will be used, regardless of how much it can store.

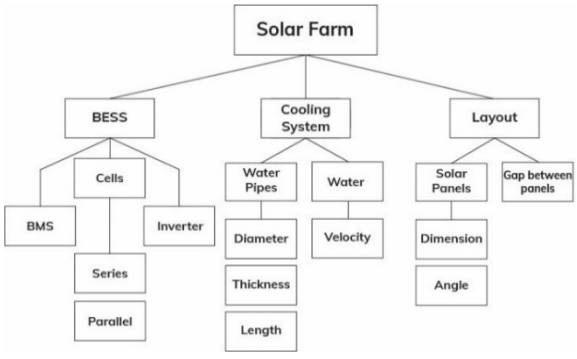

Figure 1 – A diagram displaying the component-wise system decomposition into the three subsystems

3. Subsystem 1: Battery Energy Storage System

A battery energy storage system (BESS) is a crucial part of a solar installation. It enables surplus energy to be stored and released after the sun sets, typically corelating with increased demand, dramatically improving the efficiency of the whole installation. Battery systems are expensive to install and have a limited lifecycle. Any battery installed needs to compete economically with the cost of energy from the grid over its lifecycle, otherwise it is not commercially viable to install. The battery system optimisation goal is to maximise the profit of the battery over its lifecycle.

3.1 Model Formulation

Presented is the model showing the objective function and constraints in negative null form.

$$\boldsymbol{min}\ f(x) = \Big(\big(N_s\, N_p\, P_{cell} P_{install}\big) + P_{inv}\Big) - \Big(E_{rq}\, \eta_{rt}\, P_{kWh}\, \beta_0\, DoD^{\beta_1}\ e^{\beta 2(1-DoD)}\Big)$$

$$\boldsymbol{where}\ x = (N_s, N_p, DoD, T_{cell} = [C_{Cell}, P_{cell}])$$

$$\boldsymbol{s.t.}$$

$$g_1: \quad 345539 - (3.7 N_s\, N_p\, C_{cell}\, DoD) \le 0$$

$$g_2: \quad \frac{59646}{3.7 N_s\, C_{Cell}\, N_p} - 0.5 \le 0$$

$$g_3: \quad \frac{32179}{3.7 N_s\, C_{Cell}\, N_p} - 0.5 \le 0$$

$$g_4: \quad 480 - 3.7 N_s \le 0$$

$$g_5: \quad 3.7 N_s - 324 \le 0$$

$$g_6: \quad \frac{\big(1.15\, N_s\, N_p\, P_{cell}\big) + 14000}{345539 \times 0.85 \times 0.2} - (5 \times 365) \le 0$$

$$g_7: \quad f(x) \le 0$$

$$g_8: \quad -DoD \le 0$$

$$g_9: \quad DoD - 1 \le 0$$

$$g_{10}: \quad -N_p \le 0$$

3.2 Design Variables & Parameters

Large capacity batteries are typically constructed from several smaller cells, connected in series and parallel. Adding cells in series increase the total voltage of the pack, whilst cells in parallel increases the capacity of the pack. These are managed by a battery management system (BMS) that regulates the voltage of each cell, ensuring efficient and safe operation. Battery system performance is governed by four design variables shown in table 1.

Table 1 -Table showing the design variables

Name	Notation	Unit	Type
Series Cells	N_s	Cells	Discrete Integer
Parallel Cells	N_p	Cells	Discrete Integer
Depth of discharge	DoD	%	Continuous
Cell Type	T_{cell}	n/a	Discrete

Battery cells are standardised components with fixed specifications. battery packs. The cell type effects the cell voltage, cost, capacity and safe charge/discharge rates, with cell voltage and charge/discharge rates being general values for the battery chemistry. To simplify the problem, all cells considered will be cylindrical lithium-ion cells as they are the most common type of cell used in battery packs.

Table 2 – Table showing the specifications of the selected cells

Cell	Cell Capacity (C_{cell}) / Ah	Cost (P_{cell}) / $
18650 [1]	2.6	1.10
21700 [2]	4.9	1.80
26800 [3]	6.8	9.49

Table 3 – Table containing parameters and their corresponding notation and values.

Parameter	Notation	Value
Cell Voltage [1]	V_{cell}	3.7 V
Safe Charge/Discharge Rate [1]	R_{ch} / R_{dch}	0.5C
Peak Load	E_{pk_load}	32,179 W
Peak PV Surplus	$E_{pk\_pv\_surp}$	59,646 W
Energy Required	E_{rq}	345539 Wh
DoD Coefficient 0	β_0	816.6
DoD Coefficient 1	β_1	-1.176
DoD Coefficient 2	β_2	0.0016
Round Trip Efficiency [4]	η_{rt}	0.85
Inverter minimum Voltage [5]	V_{inv_min}	324 V
Inverter Maximum Voltage [5]	V_{inv_max}	480 V
Inverter Cost [5]	P_{inv}	$14,000
Installation & Assembly Cost	$P_{install}$	1.15
Cost per kWh	P_{kWh}	$0.20

3.3 Model, Parameter & Constraint Derivations

The degradation of Li-ion cells is theorised to be a result of cracks forming in the electrode materials, this effect increases with depth of discharge [9]. A data driven metamodeling approach was adopted, as the electro-chemistry needed for a first principles derivation is outside the scope of this report. Averaged cycle data was obtained [10], and the fitnlm function in MATLAB was used to create a metamodel. Eq(1.1), a logarithmic decay function, was used as the base function, fig.xx shows the fitted model.

$$cycle\ life = \beta_0 \times DOD^{\beta_1} \times e^{\beta 2(1-DOD)} \quad (1.1)$$

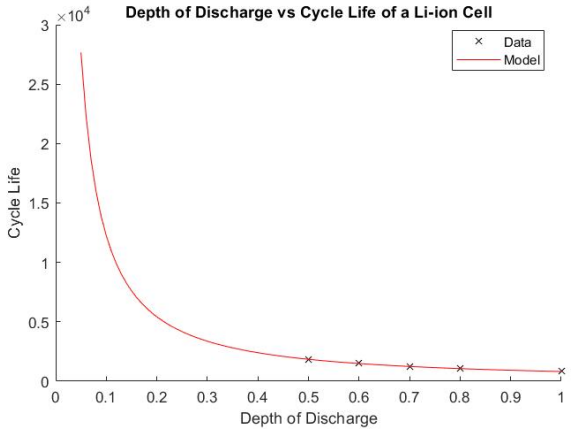

Figure 2 – graph showing the depth of discharge vs cycle life for a li-ion cell

To reduce complexity the BESS was assumed to undertake one full charge / discharge cycle per day. The residential load and solar pv output were assumed to be consistent throughout the year. The month of April as chosen as being in the spring it better approximates average annual values. Power output for a 115kWp installation in

Egypt was obtained from the PV Geographic Information System (PVGIS)[8] and a typical domestic electrical load profile was obtained from the Energy Data centre Catalogue [12]. Values for E_{pk_load}, $E_{pk\_pv\_surp}$ were obtained from combining these datasets. The value for E_{rq} was obtained by finding the area under the load curve that wasn't also under the PV generation curve. A 115kWp installation will also provide sufficient surplus output to meet the demand and account for the round-trip efficiency.

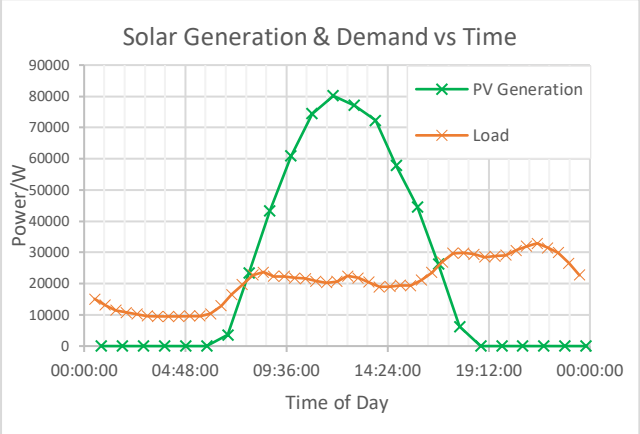

Figure 3 – graph showing averaged pv array output and averaged residential load during the month of April

To simplify the objective function, the cost of installation, assembly and the BMS have been modelled as a multiplier of 15% the total cost of the cells. The cost of the inverter is then added as can be seen in equation (1.2).

$$BESS\ cost\ = \left(N_s\, N_p\, P_{cell}\, P_{install}\right) + P_{inv} \quad (1.2)$$

The revenue the BESS generated per cycle was modelled as being equivalent to the cost of buying the same quantity energy from the grid. This is then multiplied by the expected cycle life obtained in eq(1) to create eq(3)

$$revenue = E_{rq}\, \eta_{rt}\, P_{kWh}\, \beta_0\, DoD^{\beta_1}\, e^{\beta 2(1-DoD)} \quad (1.3)$$

Table 4- table explaining and justifying the constraints.

g_x	Justification
g_1	Ensures the BESS will have enough capacity to deliver the energy required at the depth of discharge specified
g_2	Ensures the capacity is large enough to allow the surplus pv array output to charge the BESS at a safe rate and hence is able to store all the surp… gy.
g_3	Ensures the capacity is large enough to all… BESS to supply the peak load at a safe discharge rate
g_4, g_5	Constrains the BESS voltage to within the DC voltage input range of the inverter, ensuring the system will function.
g_6	Ensures the proposed BESS takes less than 5 years to break even. This constrains the exponential increase in cycle life as DoD increases and adds a practical constraint on the total cost of the installation.
g_7	Ensures the proposed BESS generates a profit
g_8, g_9	Constrains DoD as it is impossible to discharge a battery to a level greater that its capacity.
g_{10}	Ensures the number of parallel cells is positive

The profit the BESS will generate is calculated by subtracting the cost from eq(2) from the lifetime revenue calculated in eq(3) and can be seen in eq(4)

$$Profit = (E_{rq}\, \eta_{rt}\, P_{kWh}\, \beta_0\, DoD^{\beta_1}\, e^{\beta 2(1-DoD)}) - \left(\left(N_s\, N_p\, P_{cell} P_{install}\right) + P_{inv}\right) \quad (1.4)$$

3.4 Monotonicity Analysis

Initial problem exploration was conducted analytically as well as through monotonicity analysis. This showed the problem was well bounded however would need a computational solver due to the complicated non-linear constraints.

Table 5 – Table showing monotonicity analysis of the problem space

Constraint	N_s	N_p	DoD	T_{cell}
g_1	-	-	-	-
g_2	-	-		-
g_3	-	-		-
g_4	-			
g_5	+			
g_6	+	+		+
g_7	+	+	+	+
g_8			-	
g_9			+	
g_{10}		-		

3.5 Optimisation

As three of the design variables are discrete, non-gradient based genetic algorithm (GA) optimisation method was used. The Additionally, the gradient based SQP method was also used. The values for N_s & N_p were modelled as continuous and then rounded to the nearest integer for the optimal solution. To account for the discrete nature of T_{cell} the objective function implemented a rounding technique on the index of an array of the possible values. This however caused some issues discussed further in following section. Instead as there are only three cell type variable pairs, the optimiser was run once for each possibility. This was feasible due to the low computational cost of a simple objective function. The results can be found in table 6.

Table 6 – Table showing the results form the optimisation scripts run

Method	N_S	N_p	DoD	T_{Cell}	Profit
GA	99	454	0.4241	21700	24625
SQP – 18650	104	706	0.4875	N/a	4546
SQP – 21700	104	432	0.4233	N/a	24753
SQP - 26800	N/a	N/a	N/a	N/a	N/a

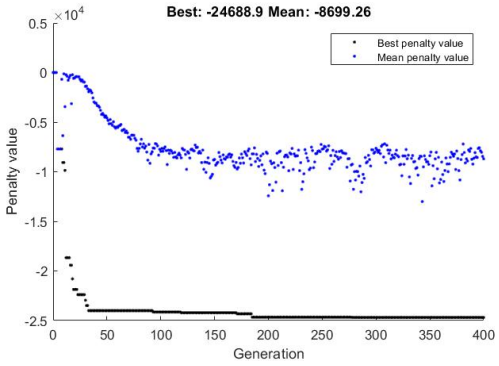

Figure 4 – Graph showing the penalty value vs generation for the GA solver

3.5 Discussion

The SQP method for the 26800 cell failed to converge on a feasible solution. This was expected as the cost per Ah of this cell is significantly larger than the other proposed cells. The rounding method applied to T_{cell} did not work, the solver struggled to deviate from the cell type allocated in the initial starting point. This is because there needed to be a 30% change in the value to see a decrease in the objective function, removing any gradient and causing the solver to see it as a stationary point.

The GA solver converged suggesting an optimum value has been found. As can be seen in figure 4 there is lots of variation. This can be explained by the fact that several N_s , N_p value combinations can yield the same value from the objective function. There is no performance trade off between N_s and N_p if they are within the required ranges. This is causing a large amount of stalling on the GA algorithm.

Both the GA and the SPQ method converged to the same value for DoD at 2s.f. As well as this optimum profit identified by each method differed by less than 1%, and the values for N_s & N_p differ by 4.8%. This increases confidence in the optimum identified.

Conclusion

The model has been simplified for the scope of this report. Solar radiation and residential load will vary each day due to weather conditional and differ considerably depending on the season. A more advanced model will be needed to accurately account for these changing conditions in future. Additionally, the range of data used for the cycle life metamodel was small. The metamodel also predicts values outside its range of training data, reducing accuracy. In future primary data could be collected through experimentation across the entire DoD range to improve the accuracy of this portion of the objective function.

Overall, the optimum BESS is made from a total of 44,928 21700 4.9Ah Li-ion cells, 104 combined in series and 432 in parallel. The BESS should be operated at a depth of discharge of 42.33%, and over the course of its lifetime is expected to make $24,753 of profit on its $107,000 cost, a margin of 23.1%.

4. Subsystem 2: Water Jacket Cooling System

The subsystem of a water jacket cooling system (12) was chosen with the aim of minimising heat flux (heat transfer per unit area) from a solar panel to water pipes. As solar panels get hotter during the day, their efficiency slowly decreases as there is an inverse relation (14) between temperature and energy efficiency.

Cooling systems are used to help the solar panels maintain their efficiency by drawing heat away from them towards cool water. This takes the form of a water jacket which is created using straight pipes with varied lengths, diameters and thicknesses and water flowing through at various speeds. Finding an efficient rate of heat flux (15) would allow solar farm owners to cut costs on variables that give the optimum cooling effect on solar panels.

4.1 Optimisation formulation

The optimisation formulation is expressed below in negative null form together with its constraints. Definitions of variables can be found in table (7).

$$min\ f\ (heat\ flux)\ or\ \varphi = 25.39x_1 + 95.2x_1^2 + 237.8x_2 + 4.753x_3 + 0.929x_4^2 - 1016.17x_4^3 + 31.16x_4^4$$

s.t.

$$g_1(x_1, x_2) = 4[0.1 * 2\pi(x3 + 0.5 * x_1)] < 2m^2$$

$$g_2(x_1, x_2, x_3) = 4x_2(\pi(0.5x_1 + x_3)^2 - \pi(0.5x_1)^2) < 3m^2$$

$$g_3(x_4) = 0.5 * 1000 * x_4 < 20\,000Pa$$

$$g_4(x_1, x_4) = 6\pi(0.5x_1) * x_4 < 200\ Ns/m^2$$

Table 7: Variables and constraints descriptions with units

Variable	Description
x_1	Diameter of water pipe (m)
x_2	Length of water pipe (m)
x_3	Thickness of water pipe (m)
x_4	Velocity of water (m/2)
g_1	Solar panel area exposed to water jacket (m^2)
g_2	Volume of all copper pipes (m^3)
g_3	Water pressure (Pa)
g_4	Water viscosity (Ns/m^2)

There are a number of assumptions made in the study. The material of the pipes is assumed to be copper throughout with a thermal conductivity of 386 W/m/K (16) and water density is taken to be $1kg/m^3$ (17). Only 10% of the circumference of the water jacket is in contact with the solar panels to extract heat. The height of the pipes is assumed to be on ground level which is why there is no potential energy (18) for the pressure calculation constraint. The concept of metamodeling is a model of a model which makes the accuracy of calculations non-ideal compared to a real-life scenario.

4.2 Model Development

A data-based metamodeling approach was used to construct the objective function between the dimensional variables and the heat flux from solar panels to water in the pipes. The design of experiment using the Latin Hypercube Sampling method (19) was adapted from Matlab's LHS code, which produced a set of 40 combinations of variables.

These input variables were parametrically input into a Solidworks thermal study of a water pipe where Finite Element Analysis was carried out to obtain values for heat flux. The metamodel data was compiled in Matlab and split into a 60:40 ratio for training and testing. A multi-variable linear regression analysis using the "mvregress" function was carried out. The results found a highest rsq value of 0.3899 which was not promising. Following this, a multi-variable non-linear analysis was carried out with a neural network using nnstart. 10 hidden layers were used in the making of this neural network and the training, validation and testing ratios were divided in a 60-20-20 ratio using the Levenberg-Marquardt training algorithm[8].

The network was trained twice before outputting results to avoid overfitting but just enough to prevent underfitting. A total R value of 0.70313 and a performance value of 0.4472 proved the neural network worked better. Upon examination of the results, it was determined the IW, LW, B1 and B2 values were too advanced to simplify to an objective function. Thus, the function "polyfitn" was

used to derive the objective function. The results of the neural network analysis are shown below in tables (8), (9) and figure (5).

Table 8: Neural Network results; no. of samples, MSE and Rsq values

	Samples	Mean Square Error	R
Training	24	2147483647.9700	0.94921
Validation	8	2147483647.8319	0.99955
Testing	8	2147483647.1148	0.28408
Total	-	-	0.70313

Table 9: Neural Network results; variable values that were too complex to create objective function

Variable	Value
x_{offset}	[0.01;0.01]
x_{gain}	[4.081;4.081]
y_{offset}	1546.7758
y_{gain}	2.1578
y_{min}	-1
B_2	0.0718

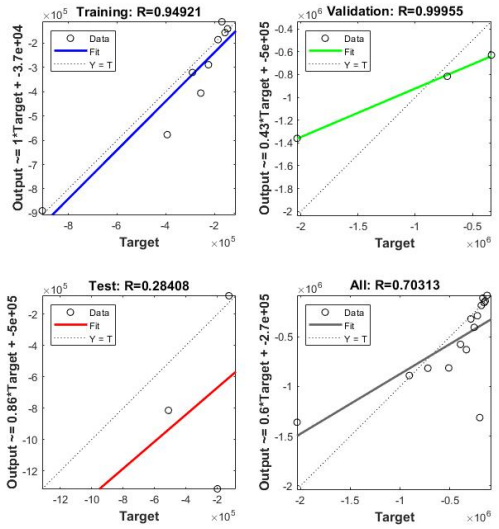

Figure 5: Neural Network results; Regression Plots (final rsq value at bottom right)

4.3 Exploring the Problem Space

Monotonicity Analysis was conducted to check which constraints were active and to simplify the model further. g_2 is used as an upper bound constraint because length of the pipe is more significant than the diameter or thickness of the pipe when considering the total circular volume which will also affect the cost required to install optimised pipes. Analysis shows that the problem is well bounded and well constrained, facilitating the use of gradient based methods for post processing optimisation.

Table 10: Monotonicity Analysis

	x_1	x_2	x_3	x_4
f	+	+	+	+
g_1			-	
g_2		-	+	
g_3				-
g_4	-			

4.4 Optimisation

As a constrained gradient-based optimisation problem, post processing was done using the GA solver and the SQP solver.

Table 11: QP and SQP solver results

	x_1	x_2	x_3	x_4
GA	0.3912	1.105	0.0316	32.481
SQP	0.3912	1.105	0.0304	32.463

The SQP solver was selected to be more ideal since its values of thickness and velocity of water are smaller allowing cost to be driven down further for the thickness of the pipe and velocity of the water while satisfying all constraints. Thickness of the pipe would have a larger impact on the total cost of purchasing multiple water jackets for a solar farm while water velocity would impact the maintenance costs slightly less. This is due to the cost of copper being significantly higher than running water. The final optimised value of heat flux for a water jacket cooling a single solar panel is $|-137930|$ W/m^2, saving the solar farm roughly £19,274 from copper to build the pipes and maintenance of water velocity.

4.5 Discussion

The objective function was found via a few indirect steps from putting the inputs and outputs through a neural network and having trained it a different number of times to average the results. Even then the nnstart functionality was too complex to understand so another function had to be used to find the objective function. In total there were 3 layers of modelling complexity, each layer decreasing in accuracy by a significant amount. It might have been easier and possibly more accurate to assume a linear regression instead despite the rsq value not being very high. Further methods to improve the optimisation process could involve more neural networks to be run and averaged out to avoid overtraining of the data to create an "ensemble model". Also, a different design of the pipes could have been considered where a single pipe which curves in an S-shape continuously such that there is only a single flow of water where different curvatures and radius of the curves could have been considered as well. Finally, more metamodeling simulations could have been done but would have taken up more time and processing power despite the limited duration of the course.

5. Subsystem 3: Solar Farm Layout

The solar farm is made up of rows of panels, installed at an angle in order to increase energy output. However, this causes shadows to be projected onto subsequent rows, which decreases efficiency.

With the compound requiring at least 500kWh of energy every day, this should be achieved by using the minimum land possible in order to reduce the cost of land or to leave space for residents. Therefore, a balance between the angle of the panels, the number or rows, distance between panels and the dimensions of the panels should be found to produce the required energy while taking up the minimum land space.

The model was constructed from first principles with five variables in the objective function and the key constraints of the minimum energy that the farm should produce.

Due to Egypt's climate, it has the least solar irradiance during winter solstice on the 21st December (24). Therefore, this date was used at 12:00 to model the position of the sun and energy relative to the farm. Specific values are in the nomenclature.

Table 12: Values used to calculate solar energy on the panels

Parameter	Value	Source
Elevation Angle, α	40.2	21
Zenith Angle, θ_z $(90-\alpha)$	49.8	21
Suns Azimuth, γ_s	180	21
Azimuth of Panels (γ)	0	23
Latitude of Farm, φ	26.4°	22
Longitude	29.9°	22
Solar declination angle, δ	-23.45°	21
Hour Angle, ω	0	21
Horizontal Beam Insolation, I	5.05 kWh/m²/day	24

5.1 Optimisation Formulation

The objective function can be optimised without knowledge from other subsystems and constraints are written in negative null form. The number or rows and width of panels are integer values.

$$\min A_f(\mathbf{x}) = \Big(D_p(N-1) + (N)(H_p)(\cos(\beta))\Big)(K)$$

$$\mathbf{x} = (D_p, N, H_p, \beta, K)$$

$$\mathbf{x} \in X \in \mathbb{R}^n$$

$$N, K \in in\ Z^+$$

$$g_1(D_p) = -D_p + 0.2 \le 0$$
$$g_2(D_p) = D_p - 1 \le 0$$
$$g_3(N) = -N + 1 \le 0$$
$$g_4(H_p) = -H_p + 1 \le 0$$
$$g_5(H_p) = H_p - 2 \le 0$$
$$g_6(\beta) = -\beta \le 0$$
$$g_7(\beta) = \beta - 90° \le 0$$
$$g_8(K) = -K + 1 \le 0$$
$$g_9(K) = K + 25 \le 0$$
$$g_{10}(D_p, N, H_p, \beta, K) = -(K)(0.2)(H_p)\Big((N-1)\big(q_{b,T}^{sh}\big) + \big(q_{b,T}\big)\Big) + 500 \le 0$$
$$g_{11}(D_p, H_p, \beta) = \frac{sin\left(49.8 - tan^{-1}\left(\frac{D_p}{H_p \sin(\beta)}\right)\right)\sqrt{{D_p}^2 + (H_p \sin(\beta))^2}}{\sin(\beta + 40.2)(H_p)} - 0.25 \le 0$$

Table 13: Variable descriptions

Variable	Symbol	Description
Distance between panel rows	D_p	Larger values decrease shading on panels to increase energy output but increase farm area.
Number of rows	N	Proportional to the area of the farm, but larger value means higher energy output.
Height of panels	H_p	Higher value increases farm area, and also can increase the shading on other panels, but cause higher energy output.
Angle of panels	β	Inversely relationship with area, but greater values cause a larger shadow, and there is an optimum so that panels are normal to sun's rays.
Width of row	K	Proportional to farm area, and also proportional to energy output

5.2 Model Development

400W solar panels of overall area 2m² (29) will be connected to make a complete panel rows of width K. The width of the farm is therefore K:

$$W_f = K$$

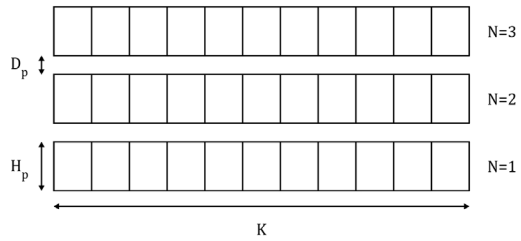

Figure 6: Arrangement of the solar panels showing 4 of the variables

The length of the farm is calculated by adding the total number of gaps in-between rows, D_p, and the 'footprint' length, H_p, of the solar panels, where N is number of rows:

$$L_f = D_p(N-1) + (N)\ (H_p)(\cos(\beta))$$

Therefore, total area of the farm is:

$$A_f = (L_f)\big(W_f\big) = (D_p(N-1) + (N)\ (H_p)(\cos(\beta)))(K)$$

The formula to calculate solar panel energy (25) can be used to calculate energy output from the first row of panels. Efficiency is calculated by the power (kW) of an individual panel over its area.

$$Q = (A\ )(r)(I)(PR)$$

$$where: \qquad r = \frac{0.4}{2}, \qquad A = (K)\big(H_p\big), \qquad I = (q_{b,T})$$

For I, only beam irradiance is considered as this is the main source of radiation (26). It is assumed that there is a performance ratio (PR) of 1 as Egypt has little cloud cover, and the losses from cables, and inverter is negligible. Therefore, the energy for the first unshaded row becomes:

$$Q = (K)(H_p)(0.2)(q_{b,T})$$

To calculate the energy term, the horizontal beam irradiance is multiplied by the relation (R_b) between irradiance on a horizontal plane and irradiance on a tilted plane (27).

$$R_b = \frac{\cos(\theta)}{\cos(\theta_z)} = \frac{0.645cos(\beta) + 0.763sin(\beta)}{0.645}$$

$$I_b = 5.05$$

$$q_{b,T} = (R_b)(I_b) = 5.05cos(\beta) + 5.98sin(\beta)$$

For the shaded rows, where there are N-1 of these, it has a different value due to the partial shading of the panels:

$$I = (q_{b,T})(1 - S) = (q_{b,T}^{sh})$$

This value is the energy term for the first row, multiplied by (1-S) where S is the fraction of shade on the solar panel as seen in the diagram.

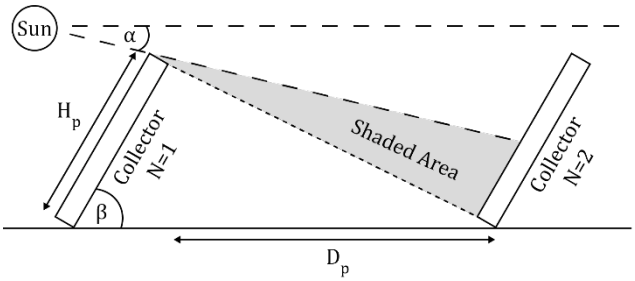

Figure 7: Showing the cause of the shade on the solar panels

The fraction of area that doesn't receive irradiance (28):

$$S = \frac{sin\left(49.8 - tan^{-1}(\frac{D_p}{H_p \sin(\beta)})\right)\sqrt{{D_p}^2 + (H_p \sin(\beta))^2}}{\sin(\beta + 40.2)(H_p)}$$

Therefore, the energy calculation for the total shaded rows is:

$$Q = (N-1)(K)(H_p)(0.2)(q_{b,T}^{sh})$$

So, the total energy (first row plus all shaded rows) is:

$$Q = (K)(0.2)(H_p)\left((N-1)(q_{b,T}^{sh}) + (q_{b,T})\right)$$

This is used as one of the most important constraints, as Q must be larger than 500kWh.

Table 14: Functional Constraint Table

Constraint	Description
$g_1, g_2(D_p)$	Panels must be at least 0.2m apart for maintenance access, and no more than 1m apart to minimize power transfer loss
$g_3(N)$	Minimum number of rows must be 1
$g_4, g_5(H_p)$	Due to manufacturing constraints, the minimum height of panels is 0.3m, and maximum is 2m.
$g_6, g_7(\beta)$	Angle of panels must be between 0 and 90 in order to face away from ground
$g_8, g_9(K)$	The maximum width of the farm was set to 25m and must be at least 1m wide.
$g_{10}(D_p, N, H_p, \beta, K)$	As the power demand is 500kWh/day this is the minimum the panels should output.
$g_{11}(D_p, H_p, \beta)$	The shade on panels should not be more than 25% so a feasible amount of panel area is used.

5.3 Exploring the Problem Space

Through monotonicity analysis, the problem was seen to be well bounded due to the variables having upper and lower bounds. The exception to this was N which only had a lower bound, but as N in the objective function is increasing in the function then g_3 will constrain it. For g_{10} and g_{10} as they are non-linear constraints it was difficult to determine whether they were active or inactive for certain variables.

Table 15: monotonicity analysis performed on the function and constraints

function	D_p	N	H_p	β	K
f	+	+	+	?	+
$g_1(D_p)$	-				
$g_2(D_p)$	+				
$g_3(N)$		-			
$g_4(H_p)$			-		
$g_5(H_p)$			+		
$g_6(\beta)$				-	
$g_7(\beta)$				+	
$g_8(K)$					-
$g_9(K)$					+
$g_{10}(D_p, N, H_p, \beta, K)$	?	-	?	?	-
$g_{11}(D_p, H_p, \beta)$	?		?	?	

5.4 Optimisation

The problem was optimised with two methods. The first was Genetic Algorithm (GA). This allows N and K to be set as discrete variables. g_{11}, g_{12} and g_{13} were set as non-linear constraints.

The second algorithm used MATLAB's 'fmincon' function through Sequential Quadratic Programming (SQP). This was used due to its robustness and effectiveness, and the problem was constrained and differentiable where post optimisation, the variables that should be discrete integer values were rounded.

Table 16: Results from the two algorithms run on the problem

Algorithm	f	D_p	N	H_p	β	K	Time(s)
GA	453	0.97	8	1.98	44.5	25	5.9
SQP	450	1	9	2	48.6	25	3.7

Post optimal analysis was carried out through sensitivity analysis. The 'fmincon' function outputted Lagrange Multipliers which showed that g_{11} was very significant with a Lagrangian of 78.6 and g_{10} was 0.2 showing that this constraint was active. The lower bound constraints (g_1, g_3, g_4, g_6, g_8) returned 0 so were inactive but 3 out of the 5 upper bounds (g_2, g_5, g_9) were active. The Lagrangian of g_9 was 1.7 which makes sense as this must be active as otherwise the farm would have all panels on the first row to eliminate any shading.

5.5 Discussion

Equations were derived to fit the global system constraints such as energy requirements and location. These were then used to formulate the optimisation which checked with monotonicity analysis. SQP and GA algorithms were then implemented to solve

this problem. In terms of the algorithm performance, SQP was faster and more reliable, however GA gave discrete values where necessary and also did not require start points so was more effective in this sense.

The largest challenge was synthesising information from different sources, where some values such as the sun's azimuth being stated as 0 degrees at south, when it should normally be measured from north. This lead to a longer time deriving the objective function as well as the non-linear constraints. To improve the optimisation problem, the sun could be modelled as moving throughout a day which would cause the shadows and energy values to change, which may affect the area. As well as this, instead of restricting the area to a quadrilateral where all the row lengths are the same and inline could be changed, where panels could be staggered and even have individual angles of tilt to ensure a steady energy supply through the whole day.

6. System Level discussion

The layout informs how far apart each solar panel should be but does not inform about the positioning of the battery and cooling subsystems.

The cooling subsystem informs us on how efficient the cooling system will be but does not inform about the efficiency of the solar panels which is more relevant to the overall solar farm.

The battery subsystem optimisation informs the system design on ideal operating parameters and composition of the BESS, for which the subsystem should run at to maximise lifecycle profit. This is a key factor in the global optimisation formulation.

However, each optimised efficiency: cost ratio is not normalised to the same scale since their variables are different from each other. It would be hard to compare types of efficiencies without understanding how they are similar.

Optimising individual subsystems does not necessarily lead to an optimised overarching system. More analysis and an overall objective function linking all the subsystems together would be more effective at determining the overall efficiency-cost ratio of a solar farm for the Egyptian village.

To optimise the system, deriving a metric to allow the comparison of each subsystem's relative efficiency-cost ratio would be beneficial. This would enable decisions on where to allocate capital to get a better global optimum to be taken. Systems hierarchy could also be used to optimise each subsystem in the order of dependencies, feeding the optimal variables of one subsystem into the parameters of another. All of this will require further system level analysis on the interdependencies and an objective function with complexity levels outside the scope of this report.

7. Conclusion

The optimum BESS parameters produced a system that will generate $24,753 of profit over its lifecycle, a margin of 23%.

While meeting the 500kwh energy demand for the compound containing 50 houses, the minimum land area required for the farm was found to be 460m^2 through optimising the angle and height of panels, as well as the number of rows and spacing of panels.

The optimum efficiency-cost ratio for the water jacket subsystem is |-137930| W/m^2 which saves £19,274 from installation and maintenance costs. Cost is calculated from excess copper used to create the pipe and water velocity maintenance averaged from water pump costs.

Overall, this study has identified a set of optimum design variables that can be used in the construction of a solar farm that enables 50 Egyptian houses to become self-sufficient in energy generation.

Breaking down a subsystem and formulating an objective function was the most challenging aspect and the most time consuming. Also, some subsystems may not pan out the way that we wanted them to. The optimisation of an individual solar panel is absent due to that subsystem being too simple and not having enough depth as a subsystem by itself and if cost is considered would require concepts out of the scope of this module.

Coordinating between each other to figure out global constraints is complicated since some subsystems would benefit from some constraint values being higher and other subsystems would benefit from those values being lower for individual subsystem efficiency: cost ratios. Early coordination and dissecting the overarching system into appropriate subsystems is essential and would have left more time for each subsystem to be explored at a deeper level, allowing for more time and for metamodeling to be developed and extended considerations for first principal derivations.

References

1. Anon (2021) Best Countries For Up And Coming Economy. *CEOWORLD magazine*. [Online]. Available from: https://ceoworld.biz/2021/03/09/best-countries-for-up-and-coming-economy/ [Accessed: 15 December 2021].

2. Anon (n.d.) *Climate and average weather in Egypt*. [Online]. World Weather & Climate Information. Available from: https://weather-and-climate.com:80/average-monthly-Rainfall-Temperature-Sunshine-in-Egypt [Accessed: 15 December 2021a].

3. Anon (n.d.) *Electricity use in homes - U.S. Energy Information Administration (EIA)*. [Online]. Available from: https://www.eia.gov/energyexplained/use-of-energy/electricity-use-in-homes.php [Accessed: 15 December 2021b].

4. Anon (n.d.) *21700 Battery 4800mah 3.7v Li-ion High Power Battery Cell - Buy 21700 Battery,4800mah 3.7v,High Power Battery Product on Alibaba.com*. [Online]. Available from: https://www.alibaba.com/product-detail/21700-battery-4800mAh-3-7V-Li_1600075040635.html?spm=a2700.galleryofferlist.normal_offer.d_title.558927edAbGOs2 [Accessed: 15 December 2021c].

5. Anon (n.d.) *Hot Sale Bulk Stock Cylindrical Lithium Ion Cell 18650 5c 3c 1c Icr 3.7v 2600mah Li-ion Rechargeable Battery - Buy 18650 Battery,Li-ion 18650,3.7v 18650 Lithium Ion Battery Product on Alibaba.com*. [Online]. Available from: https://www.alibaba.com/product-detail/Hot-Sale-Bulk-Stock-Cylindrical-Lithium_1600251702528.html?spm=a2700.galleryofferlist.normal_offer.d_title.78e374831pqnlK&s=p [Accessed: 15 December 2021d].

6. Anon (n.d.) *11.99US $ |1PCS QB26800 NEW MODEL 26800 6800MAH MODEL AIRPLANE BATTERY CELL 3.7V 5C 30A EV BATTERY|Button Cell Batteries| - AliExpress*. [Online]. aliexpress.com. Available from: //www.aliexpress.com/item/4001159473848.html?src=ibdm_d03p0558e02r02&sk=&aff_platform=&aff_trace_key=&af=&cv=&cn=&dp= [Accessed: 15 December 2021a].

7. Energy.gov. 2021. [online] Available at: <https://www.energy.gov/sites/default/files/2019/07/f65/Storage%20Cost%20and%20Performance%20Characterization%20Report_Final.pdf> [Accessed 15 December 2021].

8. Energy.gov. 2021. [online] Available at: <https://www.energy.gov/sites/default/files/2019/07/f65/Storage%20Cost%20and%20Performance%20Characterization%20Report_Final.pdf> [Accessed 15 December 2021].

9. ResearchGate. 2021. (PDF) Analysis of On-Board Photovoltaics for a Battery Electric Bus and Their Impact on Battery Lifespan. [online] Available at: <https://www.researchgate.net/publication/318292540_Analysis_of_On-Board_Photovoltaics_for_a_Battery_Electric_Bus_and_Their_Impact_on_Battery_Lifespan#pf8> [Accessed 15 December 2021].

10. Kim, T.-K. & Moon, S.-C. (2021) Novel Practical Life Cycle Prediction Method by Entropy Estimation of Li-Ion Battery. *Electronics*. [Online] 10 (4), 487. Available from: doi:10.3390/electronics10040487 [Accessed: 15 December 2021].

11. Anon (n.d.) *JRC Photovoltaic Geographical Information System (PVGIS) - European Commission*. [Online]. Available from: https://re.jrc.ec.europa.eu/pvg_tools/en/#MR [Accessed: 15 December 2021e].

12. Anon (n.d.) [Online]. Available from: https://data.ukedc.rl.ac.uk/browse/edc/efficiency/residential/LoadProfile/data [Accessed: 15 December 2021f].

13. Anon (n.d.) Cooling down PV panels with water. [Online]. pv magazine International. Available from: https://www.pv-magazine.com/2020/03/31/cooling-down-pv-panels-with-water/ [Accessed: 15 December 2021a].

14. Woo, B.C. & Lee, H.W. (2003) Relation Between Electric Power and Temperature Difference for Thermoelectric Generator. International Journal of Modern Physics B. [Online] 17 (08n09), 1421–1426. Available from: doi:10.1142/S0217979203019095 [Accessed: 15 December 2021].

15. Anon (n.d.) Heat Flux - an overview | ScienceDirect Topics. [Online]. Available from: https://www.sciencedirect.com/topics/engineering/heat-flux [Accessed: 15 December 2021b].

16. Anon (n.d.) Thermal Conductivity Coefficient - an overview | ScienceDirect Topics. [Online]. Available from: https://www.sciencedirect.com/topics/engineering/thermal-conductivity-coefficient [Accessed: 15 December 2021f].

17. Anon (n.d.) Water Density | U.S. Geological Survey. [Online]. Available from: https://www.usgs.gov/special-topics/water-science-school/science/water-density [Accessed: 15 December 2021g].

18. Anon (n.d.) potential energy | Definition, Examples, & Facts | Britannica. [Online]. Available from: https://www.britannica.com/science/potential-energy [Accessed: 15 December 2021e].

19. Anon (n.d.) Latin-Hypercube Sampling - an overview | ScienceDirect Topics. [Online]. Available from: https://www.sciencedirect.com/topics/engineering/latin-hypercube-sampling [Accessed: 15 December 2021c].

20. Anon (n.d.) Levenberg-Marquardt Algorithm - an overview | ScienceDirect Topics. [Online]. Available from: https://www.sciencedirect.com/topics/engineering/levenberg-marquardt-algorithm [Accessed: 15 December 2021d].

21. Anon (n.d.) Sun Position Calculator | PVEducation. [Online]. Available from: https://www.pveducation.org/pvcdrom/properties-of-sunlight/sun-position-calculator [Accessed: 15 December 2021d].

22. Anon (n.d.) SunCalc sun position- und sun phases calculator. [Online]. Available from: https://www.suncalc.org [Accessed: 15 December 2021e].

23. Anon (n.d.) What is the Best Angle for Solar Panels. [Online]. MPPTSOLAR. Available from: https://www.mpptsolar.com/en/best-angle-for-solar-panels.html [Accessed: 15 December 2021f].

24. Anon (n.d.) [Online]. Available from: https://www.fabhabs.com/solar-insolation-calculator [Accessed: 15 December 2021g].

25. Anon (n.d.) How to calculate output energy of PV solar systems? [Online]. Available from: https://photovoltaic-software.com/principle-ressources/how-calculate-solar-energy-power-pv-systems [Accessed: 15 December 2021b].

26. Omran, M.A. (2000) Analysis of solar radiation over Egypt. Theoretical and Applied Climatology. [Online] 67 (3), 225–240. Available from: doi:10.1007/s007040070011 [Accessed: 15 December 2021].

27. Sku.ac.ir. 2021. [online] Available at: <https://www.sku.ac.ir/Datafiles/BookLibrary/45/John%20A.%20Duffie,%20William%20A.%20Beckman(auth.)-Solar%20Engineering%20of%20Thermal%20Processes,%20Fourth%20Edition%20(2013).pdf> [Accessed 15 December 2021].

28. Harry Schlote (2021) Shading of Solar Panels. [Online]. Available from: https://www.harryschlote.com/shading-of-solar-panels [Accessed: 15 December 2021c].

29. Anon (n.d.) Amerisolar Monocrystalline Solar Panel 24V 400W AS-6M-HC Half Cell 144 PERC Cells. [Online]. Available from: https://merkasol.com/Amerisolar-Monocrystalline-Solar-Panel-AS-6M144-HC-24V-440W-Half-Cell-144-PERC-Cells [Accessed: 15 December 2021a].

Appendix

Symbol	Description	Subsystem
V_{cell}	Cell Voltage	**1**
R_{ch} / R_{dch}	Safe Charge/Discharge Rate	**1**
E_{pk_load}	Peak Load	**1**
$E_{pk\_pv\_surp}$	Peak PV Surplus	**1**
E_{rq}	Energy Required	**1**
β_0	DoD Coefficient 0	**1**
β_1	DoD Coefficient 1	**1**
β_2	DoD Coefficient 2	**1**
η_{rt}	Round Trip Efficiency	**1**
V_{inv_min}	Inverter minimum Voltage	**1**
V_{inv_max}	Inverter Maximum Voltage	**1**
P_{inv}	Inverter Cost	**1**
$P_{install}$	Installation & Assembly Cost	**1**
P_{kWh}	Cost per kWh	**1**
N_s	Series Cells	**1**
N_p	Parallel Cells	**1**
DoD	Depth of discharge	**1**
T_{cell}	Cell Type	**1**
Pa	Water pressure	**2**
m	Length	**2**
N	Force	**2**
D_p	Distance between panel rows	**3**
N	Number of rows	**3**
H_p	Height of panels	**3**
β	Angle of panels	**3**
K	Width of row	**3**
α	Elevation Angle	**3**
θ_z	Zenith Angle	**3**
γ_s	Suns Azimuth	**3**
γ	Azimuth of Panels	**3**
δ	Solar declination angle	**3**
ω	Hour Angle	**3**
I	Horizontal Beam Insolation	**3**